Discovery of a Genetic Toxin-Antidote System in Vertebrates

Duilio MZA Silva[1*], Morgan Skinner[1], Takaya Totsuka[1], Takashi Akera[1*]

[1]Cell and Developmental Biology Center, National Heart, Lung, and Blood Institute, National Institutes of Health; Bethesda, Maryland 20894, USA

*Corresponding authors. Email: duilio.silva@nih.gov, takashi.akera@nih.gov

Abstract

Toxin-antidote (TA) systems are selfish genetic elements that bias their own inheritance by coupling a toxin that kills daughter cells or offspring with an antidote that specifically rescues those with the TA. TAs are a widespread phenomenon, observed in bacteria, fungi, plants, and invertebrate animals, but have not yet been described in vertebrates. Here we report the first known vertebrate TA system that sabotages mammalian embryogenesis. The HSR locus on mouse chromosome 1 is a selfish genetic element that biases its transmission through the female germline. When HSR heterozygous females are crossed with wild-type males, wild-type embryos show high mortality, leading to preferential survival of embryos with HSR. The mechanism underlying embryo killing was unknown. We find that HSR kills wild-type post-implantation embryos by depositing a toxin (SP100) that induces significant DNA damage. Embryos with HSR also inherit the toxin but survive by expressing an antidote (SP110) that blocks the toxin's effects. Our findings reveal a previously unrecognized genetic cheating strategy in vertebrates and demonstrate its impact on mammalian reproduction.

Main

Mendel's Law of Segregation states that each parental allele is randomly transmitted to the next generation. Selfish genetic elements violate this Law by transmitting at a rate above 50% and are often accompanied by fitness costs, such as reduced fertility. Although biased transmission of selfish elements has been described in several organisms, the underlying molecular mechanisms remain elusive in most systems[1–6]. One strategy used by selfish elements is the toxin-antidote (TA) system, typically composed of a toxin and a genetically linked antidote[7,8]. Selfish DNA encodes a toxin that is distributed to all the gametes in sexually reproducing organisms or to daughter cells in bacteria and archaea. The deposited toxin impairs the development of gametes, embryos, or cells that lack the selfish element, while the ones carrying the selfish DNA survive by expressing an antidote from the TA locus. This mechanism guarantees the increased transmission of the selfish element. TA systems were initially documented four decades ago in bacteria[9,10], and many have been found in fungi, invertebrate animals, and plants[11–19]. However, TAs have yet to be described in vertebrates.

Homogeneously Staining Region (HSR) is a selfish element on mouse chromosome 1 that exhibits biased transmission, specifically through the female germline[20,21]. The HSR locus contains repetitive DNA composed of segmental duplications of at least two genes, *Sp100-rs* and *Sp110*, that are flanked by single-copy genes, *Sp100* and *Csprs,* on each end (Fig. 1a)[22]. *Sp100-rs* is a chimeric gene that arose by fusion of the 5' part of *Sp100* and *Csprs*[22]. Speckled (SP) family proteins (e.g., SP100, SP110) are chromatin readers that perform essential functions in diverse cell types and across developmental stages[23–26], although their contributions to the biased transmission of HSR remain unknown. Wild-type chromosome 1 also contains low-copy repeats (~50 copies) of these genes, but HSR at least contains 800 copies, spanning over 100 Mb (Fig. 1a)[27]. When HSR heterozygous (H/+) females are crossed with wild-type (+/+) males, roughly half of the +/+ embryos show mortality, leading to the preferential survival of H/+ embryos. This contrasts with typical selfish elements that function in the female germline, by biasing segregation to the egg[28–37], indicating that HSR uses a new mechanism of genetic cheating during mammalian reproduction.

Wild-type embryos die after implantation

A previous study reported biased transmission of the HSR locus, where chromosome 1 with HSR was part of the Robertsonian fusion with chromosome 18[20]. Therefore, it was unclear if the chromosome fusion contributed to biased transmission. It is critical to examine the contribution of Robertsonian fusion on biasd HSR transmission, especially since Robertsonian fusions can drive biased transmission in mice and humans[28,38,39]. To directly measure the strength of HSRbiased transmission, we first measured the transmission rate of the *Mus musculus domesticus* (hereafter, *dom*) HSR locus by crossing H/+ females and +/+ males (hereafter, biasing cross or BC in the Figures) and found that this locus was transmitted to 65% of the offspring, deviating from the expected Mendelian ratio (Fig. 1b and Table 1).

This biased transmission was independent of the progeny sex (Table 2). These results confirm that selfish HSR biases its transmission independently of Robertsonian fusion.

Previous characterization found that +/+ embryos from the biasing cross die between day E4.5 (blastocyst) and E11.5[20]. To precisely determine the timing of embryonic death, we dissected embryos from the biasing cross from E1.5 (two-cell) to E11.5 and genotyped them by qPCR (quantitative Polymerase Chain Reaction) and FISH (Fluorescence *in situ* Hybridization) (Fig. 1c,d). Time-course embryo collection revealed that E7.5 is the time when dead embryos at resorbing sites in the uterus are first observed (Fig. 1d-f). Interestingly, the H/+ to +/+ ratio became skewed starting at E7.5 (Fig. 1d, graph), suggesting that embryo mortality at E7.5 is the main driver of biased HSR transmission. Since mouse embryos implant at E4.5-E5.5, selfish HSR kills genetically normal embryos shortly after implantation.

Table 1. HSR transmission bias in *Mus musculus domesticus* and *Mus musculus musculus* backgrounds.

subspecies	dam genotype	sire genotype	H/+ progeny	+/+ progeny	total progeny	% H/+	*P* value
M. m. domesticus	H/+	+/+	187	100	287	65.2	<0.0001[a]
M. m. musculus	H/+	+/+	108	113	221	48.9	0.7373[a]

[a]Binomial test (two-tailed) for H/+ to +/+ ratios compared to Mendelian expectations (50:50).

Table 2. HSR transmission bias in femaloes and males of *Mus musculus domesticus*.

subspecies	dam genotype	sire genotype	H/+ females	+/+ females	total females	H/+ males	+/+ males	total males	*P* value
M. m. domesticus	H/+	+/+	103 (70.1%)	44	147	84 (60%)	56	140	0.0736[a]

[a]Chi-square test (two-tailed) for H/+ to +/+ ratios in females vs males.

Embryos die due to their internal issues

Embryos may die either due to internal issues or due to harmful interactions with the environment (i.e., external issues). Because the uterus and the dying embryos have distinct genotypes (H/+ and +/+, respectively), we wished to determine if genetic incompatibility upon implantation was responsible. We performed two distinct embryo transfer experiments. To test if an H/+ uterus can kill healthy ++ embryos, we transferred +/+ embryos that were never exposed to selfish HSR (from the +/+ x +/+ cross) to either an H/+ recipient mother or a ++ control (Fig. 1g). Transplanted embryo survival rates at E8.5, E11.5, and E17.5 were comparable between H/+ and +/+ recipient mothers (Fig. 1g). These results imply that the H/+ uterus *per se* is not toxic to +/+ embryos.

To test if biased transmission is independent of uterus genotype, we transferred a mixture of H/+ and +/+ embryos from the biasing cross to a +/+ uterus (Fig. 1h). Embryo genotyping revealed a biased genotype ratio with 63% H/+ embryos, similar to the natural biasing cross (Fig. 1h, graph), and 66.5% of the implantation sites had dead embryos, consistent with the idea that embryo death is driving the transmission bias. Thus, the H/+ uterus is not harmful for the +/+ embryos, indicating that +/+ embryos from H/+ mothers die due to internal issues.

HSR genes are overexpressed in HSR mice

To date, the only established mechanism to sabotage/kill genetically wild-type cells/embryos by internal issues is the toxin-antidote (TA) system. The HSR locus encodes several genes (*Sp100*, *Sp110*, *Sp100-rs*, and *Csprs*) (Fig. 2a) that could serve as a toxin or an antidote. In addition, the telomere-to-telomere mouse genome assembly[40] found that another SP family gene, *Sp140*, is part of HSR repeats, and our qPCR analysis confirmed that *Sp140* is indeed amplified in high-copy HSR mice (Extended Data Fig. 1). To test if these HSR genes contribute to biased transmission, we first analyzed their expression patterns by RT-qPCR (Reverse Transcription qPCR). RT-qPCR using liver tissues showed that *Sp100*, *Sp110*, and *Sp100-rs* genes were highly expressed in H/+ compared to +/+ (Fig. 2b). Intriguingly, *Sp100* shows increased expression in H/+ even though it is a single-copy gene in both genotypes. Similarly, we observed overexpression of HSR genes in H/+ oocytes compared to +/+ (Fig. 2c). The results raise a possibility that the overexpression of HSR genes mediates biased transmission by embryo killing.

No HSR gene overexpression, no biased transmission

Some meiotic drive systems in *Mus musculus domesticus* become suppressed when introduced to another subspecies, *Mus musculus musculus* (hereafter, *mus*). We tested if this applies to our system by backcrossing the HSR locus into the *mus* background for six generations and found that the HSR cheating was completely suppressed (Table 1, *M. m. musculus*). RT-qPCR analyses using *mus* liver and oocytes showed that HSR genes did not overexpress in H/+ compared to +/+ (Fig. 2d,e), consistent with the idea that HSR gene overexpression contributes to biased transmission.

The HSR locus shows a distinct C-band staining pattern[41], indicative of heterochromatin[42]. This raised the possibility that heterochromatin regulation modulates HSR gene expression profiles in *dom* vs *mus*. We examined H/+ oocytes from *dom* and *mus* by immunostaining and found that levels of histone H3K9me3, a heterochromatin marker, are significantly higher at the HSR locus in *mus* compared to *dom*, consistent with the HSR gene silencing in the *mus* background (Fig. 2f).

Toxin candidate is equally distributed to all embryos

Embryo transfer experiments and gene expression analyses imply that HSR genes regulate biased transmission, possibly through a TA system. There are at least three main requirements for a TA system to operate in the female germline: (1) the toxin needs to be produced during oogenesis and be deposited to all eggs and resulting embryos, (2) the antidote needs to function after fertilization, specifically in the embryos with the selfish element, and (3) when

135 the toxin alone is present in embryos, it must sabotage embryogenesis. It is critical to
136 examine which HSR genes satisfy these requirements to operate a TA system during
137 mammalian reproduction. A clue came from a study using human culture cells, showing that
138 SP100 overexpression led to increased DNA damage and cell death[43]. Furthermore, co-
139 expressing SP100 and SP110 prevented cell death[43]. Based on these observations, we
140 hypothesized that SP100 and SP110 could be the toxin and the antidote, respectively, in the
141 HSR system.

142 To test the toxin (SP100) – antidote (SP110) hypothesis for HSR cheating, we first examined
143 SP100 protein levels across different tissues. We found that the major isoform of the SP100
144 protein (68 kDa) is highly expressed in ovaries, compared to liver, spleen, thymus, and testis
145 (Fig. 2g and Extended Data Fig. 2). This result is consistent with the first requirement for a
146 TA system, that the toxin is produced during oogenesis. The western blot analysis also
147 showed lower SP100 levels in HSR/+ *mus* ovaries compared to *dom* (Fig. 2g, right),
148 consistent with the idea that the *mus* background suppresses the expression of HSR genes to
149 cancel biased transmission. H/+ and +/+ ovaries showed similar SP100 protein levels, but
150 ovaries are composed mostly of non-gamete cells. Therefore, we decided to analyze SP100
151 levels in more detail at a cellular level, focusing on oocytes and embryos (see below).

152 To directly visualize how the toxin candidate, SP100, is deposited in embryos, we analyzed
153 SP100 levels and its localization pattern in oocytes, eggs, and two-cell embryos. Interestingly,
154 meiosis I oocytes from H/+ females did not show higher SP100 levels compared to +/+, but
155 meiosis II eggs and two-cell embryos from H/+ females (biasing cross, BC) showed
156 increased SP100 levels compared to those from +/+ (control cross, CC) (Fig. 3a,b). SP100
157 levels were equally high in the embryos from the biasing cross regardless of embryo
158 genotype (H/+ and +/+) (Extended Data Fig. 3), consistent with the hypothesis that SP100
159 toxin is uniformly distributed to all eggs and resulting embryos when cheating happens.

160 **Antidote candidate is specifically upregulated in H/+ embryos**

161 A second requirement for a TA system is that the antidote needs to function after fertilization,
162 specifically in the embryos with the selfish element. Indeed, the antidote candidate, SP110, is
163 an established two-cell embryo marker, responding to the zygotic genome activation
164 (ZGA)[24]. This expression timing is ideal for SP110 to interact with the maternally deposited
165 toxin candidate, SP100, to suppress its toxicity. To test if embryos with selfish HSR show
166 higher SP110 levels compared to the dying +/+ embryos, we analyzed late two-cell embryos
167 that have likely completed ZGA. Our analysis showed that H/+ embryos have significantly
168 higher nuclear SP110 levels compared to +/+ embryos in the biasing cross (Fig. 3c),
169 consistent with the hypothesis. The SP110 level in +/+ embryos from the biasing cross was
170 similar to that of +/+ embryos from the control cross (Fig. 3c), suggesting that while +/+
171 embryos express basal levels of SP110, H/+ embryos overexpress SP110, likely due to their
172 higher gene-copy number, and thus neutralize the toxic effect. These results show that SP110
173 meets the requirement to serve as an antidote in the HSR system.

174 **Dying +/+ embryos have increased DNA damage**

175 A third requirement for a TA system is that a toxic effect occur in embryos when the toxin is
176 not suppressed by an antidote. Since SP100 overexpression causes increased DNA damage in
177 human cells[43], we asked if dying +/+ embryos exhibit higher DNA damage. We examined a
178 DNA damage marker, 53BP1[44], in embryonic cells from day E6.5, which is one day prior to
179 the onset of +/+ embryo death. The immunofluorescence analysis showed that +/+ embryos
180 from the biasing cross have higher levels of DNA damage compared to H/+ embryos from the
181 same cross and +/+ embryos from the control cross (Fig. 4a), raising the possibility that the
182 increased DNA damage causes the killing of +/+ embryos.

183 **SP100 and SP110 compose a minimal TA system**

184 To directly test if SP100 and SP110 are sufficient to operate a TA system during mouse
185 embryogenesis, we ectopically expressed them at various levels by microinjecting their
186 cRNA into +/+ zygotes from the control cross and cultured the embryos for three days (E3.5,
187 the morula stage) to examine the consequences on embryogenesis (Fig. 4b). We initially
188 focused on the toxin candidate, SP100, and found that SP100 overexpression is sufficient to
189 sabotage embryogenesis in a concentration-dependent manner (Fig. 4b). Overexpression at
190 the highest concentration (1,767 ng/µl) led to a complete failure of embryo development:
191 most embryos arrested at the two-cell stage and none of them reached morula (Fig. 4b). At
192 lower concentrations (90 and 125 ng/ul), 10-30% of the embryos progressed to morula,
193 although the majority of these embryos exhibited increased DNA damage (Fig. 4b, light blue
194 bars in the graph). We used these conditions to test if co-expressing SP110 rescues the toxic
195 effects. Indeed, co-expressing SP110 led to significantly reduced DNA damage (Fig. 4c) but
196 did not change the expression level of the toxin candidate, SP100 (Fig. 4c). While analyzing
197 expression levels at the two-cell stage, we noticed that some SP100-expressing embryos
198 show DNA bridges, which may be the origin or consequence of the DNA damage[45]
199 (Extended data Fig. 4). These results collectively show that SP100 and SP110, two linked
200 genes on the HSR locus, function as minimal components for the TA system.

201 We also tested whether other genes on the HSR locus, *Sp100-rs* and *Sp140*, impact
202 embryogenesis when overexpressed. While SP100-rs overexpression did not impact
203 embryogenesis (Extended Data Fig. 5a), SP140 overexpression had mild toxic effects (Fig.
204 4b), possibly contributing as a secondary toxin. The toxic effect of SP140 has also been
205 observed for the human SP140L gene[43], consistent with our observations. However, SP140
206 levels are similar between the control and biasing crosses at the two-cell embryos (Extended
207 Data Fig. 6a), suggesting that SP140 is not a primary toxin.
208

209 **Discussion**

210 We provide experimental evidence for the first canonical TA system in vertebrates that
211 sabotages mouse embryogenesis. Together with a previous study focused on a TA system in
212 *C. elegans* that delays larval development[19], we believe it is a common strategy for TA
213 systems to exploit embryogenesis. This study contributes to our understanding of how selfish
214 elements cheat and affect mammalian reproduction and raises fundamental questions
215 (discussed below).

Two linked genes, SP100 and SP110, compose a vertebrate TA system

Our HSR TA model (Fig. 4d) proposes that H/+ females poison their embryos by increasing SP100 protein levels in the egg. Higher SP100 levels kill part of the +/+ embryos with associated DNA damages while H/+ embryos survive by expressing SP110 protein, which likely interacts with SP100 to prevent DNA damages. *Sp110* starts expressing at the two-cell stage, which is an ideal timing to specifically rescue the embryos with HSR. As shown in other TA systems, toxin levels must be precisely controlled not to harm all embryos[2,7]. Indeed, extreme overexpression of SP100 arrests embryogenesis at a much earlier stage than in the natural HSR system (Fig. 4b). Also, +/+ embryos express SP110 at a basal level that would provide some protection against the toxin. This explains why some +/+ embryos survive in the biasing cross.

Intriguingly, the SP100 protein level is higher in meiosis II eggs from H/+ females compared to those from +/+ females, while it is comparable in late prophase I oocytes (Fig. 3a,b). Some mRNAs that are critical for oocyte maturation and early development exhibit dormancy in oocytes and only initiate translation in eggs and embryos[46]. *Sp100* mRNA may be employing a similar mechanism to produce toxin at the right place at the right time. Elucidating the molecular mechanism underlying the toxin production is an important future direction.

Timing control of toxic effects

Our results imply that wild-type embryos die due to increased DNA damage. Another important question is why the SP100 toxin, which is already expressed at a higher level in two-cell embryos, kills wild-type embryos only at day E6.5 – 7.5. We speculate on two possibilities. First, SP100 may lack critical cofactors to induce DNA damage during early embryogenesis. Indeed, human SP100 requires a nuclear body, the PML body, to induce DNA damage[43], and the PML body is absent from oocytes and early embryos and only starts forming at the morula stage[47]. This delayed formation of the PML body explains why SP100 does not immediately kill embryos after fertilization. We find that SP100 ectopic expression at a very high level leads to embryogenesis arrest (Fig. 4b). Thus, at a higher expression level, SP100 may be capable of killing embryos independently of the PML body.

Second, SP100 may cause mild DNA damage in early embryos, which only triggers death after implantation. Consistent with this model, previous work has shown that embryos become particularly sensitive to mild DNA damage, resulting in apoptosis at E6.5 when gastrulation takes place with high proliferation and differentiation rates[48]. Furthermore, multiple mutant mouse lines that undergo increased DNA damages during embryogenesis show lethality at E6.5 – E7.5[48–52], consistent with our model that HSR kills embryos via DNA damage.

Possible evolutionary history of HSR

HSR does not exhibit biased transmission when introduced into the *M. m. musculus* background, where HSR genes are silenced, likely by extensive heterochromatin formation (Table 1 and Fig. 2)[53]. Some *M. m. musculus* populations have another type of HSR element called double-band HSR, composed of two conspicuous heterochromatic bands originating

from a paracentric inversion involving the HSR locus. Remarkably, double-band HSR cheats during meiosis by biased segregation to the egg[54,55]. These observations raise an intriguing possibility that HSR escaped the suppression in *M. m. musculus* by evolving a new cheating strategy in a distinct arena: asymmetric female meiosis.

First known TA system in vertebrates

TA systems have been extensively studied in multiple species, since their discovery in *Escherichia coli* in 1983[9]. Although the t-haplotype meiotic drive system in male mice has occasionally been categorized as a TA-like system, it involves multiple distorters and a responder, and therefore mechanistically, it is a distorter-responder system. In contrast, HSR employs a tightly linked two-gene toxin-antidote module, characteristic of a canonical TA system. It has been shown that SP proteins, including SP100 and SP110, heterodimerize through their CARD (Caspase Activation and Recruitment Domain) domain (or HSR domain), and the SP100-SP110 interaction via the CARD domain appears to be crucial for neutralizing the cytotoxicity of SP100 overexpression[43]. Neutralization through the toxin-antidote direct interaction is another feature of canonical TA systems. Therefore, we believe HSR represents the first known canonical TA system in vertebrates.

TA systems can cause intragenomic conflict between the selfish element and the rest of the genome, facilitating genome evolution. Therefore, investigating the HSR TA system would also provide a unique window to elucidate how TA systems have shaped the mammalian genome and sexual reproduction.

Limitation of the study: Although we distinguish *Sp100* and *Sp100-rs* mRNA in RT-qPCR experiments, the SP100 antibody used in the study likely detects not only SP100 but also SP100-rs (if it is expressed as a protein). Therefore, immunofluorescence signals in Fig. 3a,b could also be originating from SP100-rs. However, since SP100-rs has lost the C-terminal portion of SP100, which includes the nuclear localization signal (NLS) (Extended Data Fig. 6b), it localizes uniformly in the embryo when expressed as a GFP-fusion construct (Extended Data Fig. 5b). Therefore, we consider that the increased nuclear enrichment of SP100 in embryos from H/+ females is indeed the full-length SP100 with NLS and not SP100-rs (Fig. 3b).

References

1. Lindholm, A. K. *et al.* The ecology and evolutionary dynamics of meiotic drive. *Trends Ecol. Evol.* **31**, 315–326 (2016).
2. Kruger, A. N. & Mueller, J. L. Mechanisms of meiotic drive in symmetric and asymmetric meiosis. *Cell. Mol. Life Sci.* **78**, 3205–3218 (2021).
3. Clark, F. E. & Akera, T. Unravelling the mystery of female meiotic drive: where we are. *Open Biol.* **11**, 210074 (2021).
4. Arora, U. P. & Dumont, B. L. Meiotic drive in house mice: mechanisms, consequences, and insights for human biology. *Chromosome Res. Int. J. Mol. Supramol. Evol. Asp. Chromosome Biol.* **30**, 165–186 (2022).

5. Chmátal, L., Schultz, R. M., Black, B. E. & Lampson, M. A. Cell biology of cheating—Transmission of centromeres and other selfish elements through asymmetric meiosis. in *Centromeres and kinetochores: Discovering the molecular mechanisms underlying chromosome inheritance* (ed. Black, B. E.) 377–396 (Springer International Publishing, Cham, 2017).
6. Helleu, Q., Gérard, P. R. & Montchamp-Moreau, C. Sex chromosome drive. *Cold Spring Harb. Perspect. Biol.* **7**, a017616 (2014).
7. Burga, A., Ben-David, E. & Kruglyak, L. Toxin-Antidote elements across the tree of life. *Annu. Rev. Genet.* **54**, 387–415 (2020).
8. LeRoux, M. & Laub, M. T. Toxin-Antitoxin systems as phage defense elements. *Annu. Rev. Microbiol.* **76**, 21–43 (2022).
9. Ogura, T. & Hiraga, S. Partition mechanism of F plasmid: Two plasmid gene-encoded products and a cis-acting region are involved in partition. *Cell* **32**, 351–360 (1983).
10. Gerdes, K., Rasmussen, P. B. & Molin, S. Unique type of plasmid maintenance function: postsegregational killing of plasmid-free cells. *Proc. Natl. Acad. Sci.* **83**, 3116–3120 (1986).
11. Beeman, R. W. & Friesen, K. S. Properties and natural occurrence of maternal-effect selfish genes ('Medea' factors) in the Red Flour Beetle, *Tribolium castaneum*. *Heredity* **82**, 529–534 (1999).
12. Beeman, R. W., Friesen, K. S. & Denell, R. E. Maternal-effect selfish genes in flour beetles. *Science* **256**, 89–92 (1992).
13. Seidel, H. S. *et al.* A Novel Sperm-delivered toxin causes late-stage embryo lethality and transmission ratio distortion in *C. elegans*. *PLoS Biol.* **9**, e1001115 (2011).
14. Turner, B. C. & Perkins, D. D. Spore killer, a chromosomal factor in *Neurospora* that kills meiotic products not containing it. *Genetics* **93**, 587–606 (1979).
15. Rhoades, N. A. *et al.* Identification of rfk-1, a meiotic driver undergoing RNA editing in *Neurospora*. *Genetics* **212**, 93–110 (2019).
16. Nuckolls, N. L. *et al.* wtf genes are prolific dual poison-antidote meiotic drivers. *eLife* **6**, e26033 (2017).
17. Yang, J. *et al.* A killer-protector system regulates both hybrid sterility and segregation distortion in rice. *Science* **337**, 1336–1340 (2012).
18. Ben-David, E., Burga, A. & Kruglyak, L. A maternal-effect selfish genetic element in *Caenorhabditis elegans*. *Science* **356**, 1051–1055 (2017).
19. Pliota, P. *et al.* Selfish conflict underlies RNA-mediated parent-of-origin effects. *Nature* **628**, 122–129 (2024).
20. Weichenhan, D., Traut, W., Kunze, B. & Winking, H. Distortion of Mendelian recovery ratio for a mouse HSR is caused by maternal and zygotic effects. *Genet. Res.* **68**, 125–129 (1996).
21. Traut, W., Winking, H. & Adolph, S. An extra segment in chromosome 1 of wild *Mus musculus*: a C-band positive homogeneously staining region. *Cytogenet. Cell Genet.* **38**, 290–297 (1984).
22. Traut, W., Rahn, I. M., Winking, H., Kunze, B. & Weichenhan, D. Evolution of a 6–200 Mb long-range repeat cluster in the genus *Mus*. *Chromosoma* **110**, 247–252 (2001).
23. Fraschilla, I. & Jeffrey, K. L. The Speckled Protein (SP) Family: Immunity's chromatin readers. *Trends Immunol.* **41**, 572–585 (2020).
24. Guo, Y. *et al. Obox4* promotes zygotic genome activation upon loss of *Dux*. *eLife* **13**, e95856 (2024).
25. Witt, K. C. *et al.* SP140–RESIST pathway regulates interferon mRNA stability and antiviral immunity. *Nature* **643**, 1372–1380 (2025).

26. Ji, D. X. *et al.* Role of the transcriptional regulator SP140 in resistance to bacterial infections via repression of type I interferons. *eLife* **10**, e67290 (2021).
27. Agulnik, S., Plass, C., Traut, W. & Winking, H. Evolution of a long-range repeat family in chromosome 1 of the genus *Mus*. *Mamm. Genome* **4**, 704–710 (1993).
28. Chmátal, L. *et al.* Centromere strength provides the cell biological basis for meiotic drive and karyotype evolution in mice. *Curr. Biol.* **24**, 2295–2300 (2014).
29. Iwata-Otsubo, A. *et al.* Expanded satellite repeats amplify a discrete CENP-A nucleosome assembly site on chromosomes that drive in female meiosis. *Curr. Biol. CB* **27**, 2365-2373.e8 (2017).
30. Akera, T. *et al.* Spindle asymmetry drives non-Mendelian chromosome segregation. *Science* **358**, 668–672 (2017).
31. Wu, T., Lane, S. I. R., Morgan, S. L. & Jones, K. T. Spindle tubulin and MTOC asymmetries may explain meiotic drive in oocytes. *Nat. Commun.* **9**, 2952 (2018).
32. Dawe, R. K. *et al.* A Kinesin-14 motor activates neocentromeres to promote meiotic drive in maize. *Cell* **173**, 839-850.e18 (2018).
33. Didion, J. P. *et al.* A Multi-megabase copy number gain causes maternal transmission ratio distortion on mouse chromosome 2. *PLOS Genet.* **11**, e1004850 (2015).
34. Fishman, L. & Saunders, A. Centromere-associated female meiotic drive entails male fitness costs in monkeyflowers. *Science* **322**, 1559–1562 (2008).
35. Hanlon, S. L. & Hawley, R. S. B chromosomes reveal a female meiotic drive suppression system in *Drosophila melanogaster*. *Curr. Biol.* **33**, 2300-2306.e5 (2023).
36. Clark, F. E. & Kocher, T. D. Changing sex for selfish gain: B chromosomes of Lake Malawi cichlid fish. *Sci. Rep.* **9**, 20213 (2019).
37. Hewitt, G. M. Meiotic drive for B-chromosomes in the primary oocytes of *Myrmekotettix maculatus* (Orthoptera: Acrididae). *Chromosoma* **56**, 381–391 (1976).
38. Gropp, A. *et al.* Robertsonian karyotype variation in wild house mice from Rhaeto-Lombardia. *Cytogenet. Cell Genet.* **34**, 67–77 (2008).
39. Pardo-Manuel de Villena, F. & Sapienza, C. Female meiosis drives karyotypic evolution in mammals. *Genetics* **159**, 1179–1189 (2001).
40. Francis, B. A. *et al.* Complete genome assemblies of two mouse subspecies reveal structural diversity of telomeres and centromeres. *Nat. Genet.* **57**, 2852–2862 (2025).
41. Winking, H. *et al.* Polymorphic HSRs in chromosome 1 of the two semispecies *Mus musculus musculus* and *M. m. domesticus* have a common origin in an ancestral population. *Chromosoma* **100**, 147–151 (1991).
42. Sumner, A. T. A simple technique for demonstrating centromeric heterochromatin. *Exp. Cell Res.* **75**, 304–306 (1972).
43. Aird, E. J. *et al.* SP110 sequestration of SP100 protects against toxic filaments during innate immune signaling. 2024.04.03.587867 Preprint at https://doi.org/10.1101/2024.04.03.587867 (2024).
44. Paiano, J. *et al.* Role of 53BP1 in end protection and DNA synthesis at DNA breaks. *Genes Dev.* **35**, 1356–1367 (2021).
45. Lukas, C. *et al.* 53BP1 nuclear bodies form around DNA lesions generated by mitotic transmission of chromosomes under replication stress. *Nat. Cell Biol.* **13**, 243–253 (2011).
46. Lorenzo-Orts, L. & Pauli, A. The molecular mechanisms underpinning maternal mRNA dormancy. *Biochem. Soc. Trans.* **52**, 861–871 (2024).
47. Udagawa, O., Kato-Udagawa, A. & Hirano, S. Behavior of assembled promyelocytic leukemia nuclear bodies upon asymmetric division in mouse oocytes. *Int. J. Mol. Sci.* **25**, (2024).

48. Heyer, B. S., MacAuley, A., Behrendtsen, O. & Werb, Z. Hypersensitivity to DNA damage leads to increased apoptosis during early mouse development. *Genes Dev.* **14**, 2072–2084 (2000).
49. Tebbs, R. S. *et al.* Requirement for the *Xrcc1* DNA base excision repair gene during early mouse development. *Dev. Biol.* **208**, 513–529 (1999).
50. Gurley, K. E. & Kemp, C. J. Synthetic lethality between mutation in Atm and DNA-PKcs during murine embryogenesis. *Curr. Biol.* **11**, 191–194 (2001).
51. Henrie, M. S. *et al.* Lethality in PARP-1/Ku80 double mutant mice reveals physiological synergy during early embryogenesis. *DNA Repair* **2**, 151–158 (2003).
52. Juan, H.-C., Lin, Y., Chen, H.-R. & Fann, M.-J. Cdk12 is essential for embryonic development and the maintenance of genomic stability. *Cell Death Differ.* **23**, 1038–1048 (2016).
53. Torgunakov, N. Y. *et al.* Homogeneously Staining Regions (HSR) in chromosome 1 of the house mouse: synapsis and recombination at meiosis. *Cytogenet. Genome Res.* **161**, 14–22 (2021).
54. Agulnik, S. I., Sabantsev, I. D., Orlova, G. V. & Ruvinsky, A. O. Meiotic drive on aberrant chromosome 1 in the mouse is determined by a linked distorter. *Genet. Res.* **61**, 91–96 (1993).
55. Agulnik, S. I., Agulnik, A. I. & Ruvinsky, A. O. Meiotic drive in female mice heterozygous for the HSR inserts on chromosome 1. *Genet. Res.* **55**, 97–100 (1990).
56. Behringer, R., Gertsenstein, M., Nagy, K. V. & Nagy, A. Assisted reproduction. in *Manipulating the Mouse Embryo: A Laboratory Manual* 608–613 (Cold Spring Harbor Laboratory Press, 2014).
57. Shea, K. & Geijsen, N. Dissection of 6.5 dpc Mouse Embryos. *J. Vis. Exp. JoVE* 160 (2007) doi:10.3791/160.
58. Truett, G. E. *et al.* Preparation of PCR-quality mouse genomic DNA with Hot Sodium Hydroxide and Tris (HotSHOT). *BioTechniques* **29**, 52–54 (2000).
59. Bel, Y., Ferré, J. & Escriche, B. Quantitative real-time PCR with SYBR Green detection to assess gene duplication in insects: study of gene dosage in *Drosophila melanogaster* (Diptera) and in *Ostrinia nubilalis* (Lepidoptera). *BMC Res. Notes* **4**, 84 (2011).
60. Kõressaar, T. *et al.* Primer3_masker: integrating masking of template sequence with primer design software. *Bioinformatics* **34**, 1937–1938 (2018).
61. Dozortsev, D. I. & McGinnis, K. T. An improved fixation technique for fluorescence *in situ* hybridization for preimplantation genetic diagnosis. *Fertil. Steril.* **76**, 186–188 (2001).
62. Yu, G. *et al.* Application of improved single blastomere fixation technique in preimplantation genetic diagnosis. *Cytotechnology* **72**, 217–226 (2020).
63. Clark, F. E. *et al.* Whole mount oligopaint fluorescence in situ hybridization of mouse oocytes, eggs, or early-stage embryos. in *Mammalian Oocyte Development* 69–86 (Humana New York, 2025).
64. Igarashi, H., Knott, J. G., Schultz, R. M. & Williams, C. J. Alterations of PLCβ1 in mouse eggs change calcium oscillatory behavior following fertilization. *Dev. Biol.* **312**, 321–330 (2007).
65. Ye, J. *et al.* Primer-BLAST: A tool to design target-specific primers for polymerase chain reaction. *BMC Bioinformatics* **13**, 134 (2012).
66. Kubista, M. & Sindelka, R. The Prime Technique. *GIT Lab J Eur* 33 (2007).
67. Livak, K. J. & Schmittgen, T. D. Analysis of Relative Gene Expression Data Using Real-Time Quantitative PCR and the $2^{-\Delta\Delta CT}$ Method. *Methods* **25**, 402–408 (2001).
68. Xie, F., Wang, J. & Zhang, B. RefFinder: a web-based tool for comprehensively analyzing and identifying reference genes. *Funct. Integr. Genomics* **23**, 125 (2023).

69. Weichenhan, D. *et al.* Source and component genes of a 6–200 Mb gene cluster in the house mouse. *Mamm. Genome* **12**, 590–594 (2001).

Methods

Mouse strains and crossing schemes

Mouse strains were purchased from the Jackson Laboratory (B6.Cg-Is(HSR;1)1Lub/J, stock# 001914, *Mus musculus domesticus* with the HSR locus on chromosome 1, C57BL/6J, stock# 000664, *Mus musculus domesticus*, PWD/PhJ, stock# 004660, *Mus musculus musculus*) or Charles River (CD-1® IGS, stock# 022, *Mus musculus domesticus*). The HSR locus was introduced to the *M. m. musculus* background by backcrossing H/+ *M. m. domesticus* mice with +/+ *M. m. musculus* (PWD/PhJ) mice for six generations. HSR transmission was measured by crossing H/+ *dom* females and +/+ *dom* males or by crossing H/+ *mus* females from the backcrosses and +/+ *mus* males. Mice were maintained in an animal facility under a 12-hour light/dark cycle at room temperature, with minimal disturbance and humidity ranging from 30% to 70% depending on the season. All animal experiments were conducted in accordance with the National Institutes of Health guidelines and approved by the Animal Care and Use Committee (Animal Study Proposal Numbers: H-0327 and H-0125).

Mouse oocyte and egg collection and culture

For oocyte collection, 6-12 week old *M. m. domesticus* females were primed with 7.5 U of pregnant mare serum gonadotropin (PMSG, Medix Biochemica, cat# 493-10) 44-48 hour before collection, while *M. m. musculus* females were primed with 5 U of CARD HyperOva (Cosmo Bio, cat# KYD-010-06-EX) 44-48 hour before collection. For metaphase II egg collection, the females were also primed with 7.5 IU of hCG (Millipore, Cat# 9002–61-3 C1063) 48 hours after the PMSG injection and euthanized 17 hours after the hCG injection. Germinal vesicle (GV) oocytes were collected in M2 media (Sigma, cat# M7167) with 2.5 mM milrinone (Sigma, cat# 475840) to inhibit meiotic resumption. Oocytes were then transferred to M16 media (Millipore, cat# M7292) with 2.5 mM milrinone covered with parafin oil (Nacalai, cat# NC1506764) in a humidified atmosphere of 5% CO_2 in air at 37°C. For prometaphase I analysis (Fig. 2f), milrinone was washed out to allow meiotic resumption. The oocytes were then fixed 3 hours after milrinone washout. Eggs were collected in M2 media from the ampulla of 4-12 week old females, transferred to M16 media covered with paraffin oil, and incubated at 37°C in a humidified atmosphere of 5% CO_2 in air. Oocyte and egg manipulations were performed in an Petri dish (Falcon, cat# 351007).

In vitro fertilization to obtain zygotes

Zygotes were obtained by IVF following the Nakagata method[56], using +/+ *dom* sperm and H/+ or +/+ *dom* eggs, except that eggs were collected in HTF media (Millipore, cat# MR-070-D). Cumulus cells and sperm were washed out 4-6 hours after fertilization in HTF media, and zygotes were transferred to KSOM media (Millipore, cat# MR-106) under paraffin oil. Zygote pronuclei were examined with an M80 stereo microscope (Leica, cat# 01-672-670) with a Thermo Plate TPX (Leica). Embryos with anormal pronuclei numbers and unfertilized

486 eggs were discarded. Zygotes were cultured at 37°C in a humidified atmosphere of 5%
487 CO_2 in air to reach various stages.

488 Post-implantation embryo collection

489 Embryos were dissected from H/+ *dom* pregnant females naturally mated with +/+ *dom*
490 males. Dissections were performed during embryonic days E6.5 to E11.5 following standard
491 laboratory protocols[56,57]. Embryos were placed in HBSS media (Gibco, cat# 14175095) and
492 imaged using the MZ16F stereomicroscope (Leica) and the Leica Application Suite X
493 software. After imaging, embryos were frozen at -70°C until genotyping (see below).

494 DNA isolation and genotyping by qPCR

495 Genomic DNA (gDNA) was extracted from tail snips following the HotSHOT protocol[58].
496 Samples were genotyped by measuring the relative quantification (RQ) of the *Sp100-rs* gene
497 by qPCR. RQ was estimated through the $2^{-\Delta C_T}$ method[59] using the *36b4* gene as a reference
498 (Supplementary Table 1). Primers were designed using a modified version of Primer3 2.3.7[60]
499 implemented in Geneious 10.2.6 (Biomatters) (Supplementary Table 1). The presence of the
500 *Sp140* gene in the HSR locus was also tested with a specific primer set (Supplementary Table
501 1) using the *36b4* gene as a reference. Quantitative PCR was performed on a LightCycler 96
502 (Roche). Reactions were performed at a final volume of 10 µL, with 60 ng of gDNA, 5 µL of
503 iTaq Universal SYBR Green Supmix (Bio-Rad, cat# 1725121), and 1 µL of each 5 µM
504 primer. Cycle conditions were 95°C for 10 min; 40 cycles of 95°C for 5 s and 60°C for 20 s.
505 Target and reference genes were analyzed simultaneously in triplicate. The specificity of the
506 PCR products was confirmed by dissociation curve analysis. We estimated the amplification
507 efficiency (E) of each primer set by standard curve performed on a 5-fold dilution series of
508 gDNA. Amplification efficiencies were E*Sp100-rs* = 100% and E*36b4* = 96%, which are
509 acceptable to use for the $2^{-\Delta C_T}$ method without correction. We classified animals as wild-type,
510 heterozygous for HSR, and homozygous for HSR, comparing their RQ values with those
511 obtained from animals with known genotypes. Animals with inconsistent RQ values were
512 excluded from any following experiments. E1.5 to E7.5 embryos were genotyped by FISH
513 using an HSR probe (see below).

514 Oligopaint design and genotyping by FISH

515 We manually designed a set of probes for the HSR locus. Probes were designed at the
516 *Sp100-rs* and *Sp110* exons and were synthesized by Integrated DNA Technologies. E1.5-E4.5
517 embryos produced by natural crosses were spread onto microscope slides based on the
518 standard protocol[61,62]. Briefly, embryos were treated with a hypotonic solution (0.1% sodium
519 citrate in 0.2 mg/ml BSA), transferred to a hypotonic solution drop onto the microscope slide,
520 and air dried. Just before completely dried, 8 µL of spreading solution (0.1% Tween-20 in
521 0.01 N HCl) was added over the cells and allowed to dry for about 1 hour. Cells were then
522 fixed using a 1:3 mixture of acetic acid/methanol and let air dry. The FISH process was
523 performed following the procedures described in Clark et al[63] using 100 pmol of the HSR
524 primary probe. E6.5 and E7.5 embryos were spread and genotyped by FISH as described in
525 "Immunostaining and FISH on E6.5 embryos" (see below).

526 Western blot

527 Liver, ovary, testis, thymus, and spleen samples were dissected, flash frozen in liquid
528 nitrogen, and stored at -70°C. To extract protein from dissected tissues, 50 mg of each sample
529 were homogenized using RIPA buffer (150 mM NaCl (Millipore, cat# 116224), 0.5% Sodium
530 deoxycholate (Biochemica, cat# A1531), and 50 mM Tris, pH 8.0 (KD Medical, cat# RGF-
531 3360), and 1% Triton X-100) supplemented with the protease inhibitor cocktail (MedChem
532 Express, cat# HY-K0010). Extracts were mixed with Laemmli buffer (BioRad, cat# 1610737)
533 containing 2-mercaptoethanol (VWR Life Sciences, cat# 97064-590) and denatured at 95°C
534 for 5 min. Samples were separated on 10% Mini-Protean TGX Stain-Free Protein Gels (Bio-
535 Rad, cat# 4568035) to visualize the total proteins with the ChemiDoc MP Imaging System
536 (Bio-Rad, cat# 12003154). Proteins were then transferred to the PVDF membrane (Bio-Rad,
537 cat# 1704156) with the Trans-Blot Turbo System (Bio-Rad, cat# 1704150). The membrane
538 was blocked for 1 hour at RT with 2% Membrane Blocking agent (Cytiva, cat# RPN2125),
539 incubated overnight at 4°C with the mouse anti-human SP100 (1:1000, Santa Cruz, cat# sc-
540 293458), and washed three times for 15 min each with the TBST buffer (20 mM Tris, pH 7.6,
541 150 mM NaCl, and 0.1% Tween-20). The membrane was then incubated for 1 hour with the
542 Goat Anti-Mouse IgG-heavy and light chain cross-adsorbed Antibody HRP conjugated
543 (1:10,000 Bethyl, cat# A90-516P), followed by three 15 min washes with the TBST buffer.
544 SP100 protein was visualized using the ECL detection reagents (Bio-Rad, cat# 1705062) and
545 ChemiDoc MP Imaging System.

546 Immunostaining of whole oocytes, eggs, and two-cell embryos

547 Oocytes at the germinal vesicle stage (GV) or prometaphase I (3 hour from milrinone
548 washout), meiosis II eggs, and early two-cell embryos were fixed in freshly prepared 2%
549 paraformaldehyde (Electron Microscopy Sciences, cat# 15710) in 1x PBS (Quality
550 Biological, cat# 119-069-101CS) with 0.1% Triton X-100 (Millipore, cat# TX1568–1) for 20
551 min at room temperature (RT), washed in blocking solution (0.3% BSA (Fisher bioreagents,
552 cat# BP1600–100) and 0.01% Tween-20 (ThermoFisher, cat# J20605-AP) in 1x PBS) for 10
553 min at RT, permeabilized in 1x PBS with 0.1% Triton X-100 for 15 min at RT, incubated in
554 the blocking solution for 15 min at RT, incubated for 1 hour with primary antibodies at RT,
555 washed three times for 10 min with the blocking solution, incubated for 1 hour with
556 secondary antibodies at RT, and washed three times for 10 min in the blocking solution. GV
557 oocytes, eggs, and two-cell embryos were incubated for 30 min with Antifade Mounting
558 Medium with DAPI (Vector Laboratories, cat# H-1200) diluted 1:1 in the blocking solution
559 and placed into 3 µl drops of the blocking solution covered with paraffin oil in a glass-bottom
560 tissue culture dish (fluoroDish, cat# FD35–100). Oocytes at prometaphase I were mounted on
561 microscope slides with Antifade Mounting Medium with DAPI. The following primary
562 antibodies were used: rabbit anti-mouse SP100 antibody (Fig. 3a, b and Extended Data Fig. 3,
563 1:100, custom serum raised by LabCorp), rabbit anti-human SP140 antibody (Extended Data
564 Fig. 6a, 1:100, Invitrogen, cat# PA5-110417), and rabbit anti-mouse H3K9me3 antibody (Fig.
565 2f, 1:100, Abcam, cat# ab8898). Secondary antibodies used were Alexa Fluor 488–
566 conjugated donkey anti-rabbit (1:500, Invitrogen, cat# A21206), and Alexa Fluor 568–
567 conjugated donkey anti-rabbit (1:500, Invitrogen, cat# A10042).

568 Immunostaining and Oligopaint FISH of mouse oocytes and embryos

569 Immunostaining combined with FISH for mouse oocytes and two-cell embryos followed our
570 recently developed protocol[63]. Briefly, prometaphase I oocytes and two-cell embryos were
571 immunostained with rabbit anti-mouse H3K9me3 antibody (Fig. 2f, 1:100, Abcam, cat#
572 ab8898) and Alexa Fluor 568–conjugated donkey anti-rabbit (1:500, Invitrogen, cat#
573 A10042) secondary antibody. Two-cell embryos were immunostained with mouse anti-mouse
574 SP110 (Fig. 3c, 1:33, Santa Cruz, cat# sc-376345) or rabbit anti-mouse SP100 antibody
575 (Extended Data Fig. 3, 1:100, custom serum raised by LabCorp) as a primary antibody and
576 Alexa Fluor 488–conjugated donkey anti-rabbit (1:500, Invitrogen, cat# A21206) or Alexa
577 Fluor 488–conjugated donkey anti-mouse (1:500, Invitrogen, cat# A21202) as a secondary
578 antibody. Embryos were incubated overnight at 4°C in the primary antibody for the SP110
579 staining or 1 hour at RT for the SP100 staining. The blocking solution used for this
580 immunostaining was (0.3% BSA and 0.01% Tween-20 in 1x PBS). Subsequent FISH used
581 100 pmol of the HSR probe. To improve the retention rate of embryos on the microscope
582 slide, we made the following modification to the original protocol[63]. Prior to attaching
583 embryos to the slide, embryos were washed in 1x PBS in ultra-low attachment microplates
584 (Corning Costar, cat# 07-200-601) to prevent adhesion to the dish. Embryos were then
585 transferred to a 1x PBS drop on Fisherbrand ColorFrost Plus microscope slides (Fisher
586 Scientific, cat# 12-550-16A), instead of poly-L-lysine treated slides[63], allowing them to
587 attach. After PFA fixation[63], slides were washed three times for 5 min with 10 ml of 1x PBS
588 while placing the slides horizontally on the bench (instead of inserting them vertically into
589 cuplin jar), which minimizes embryo detachment from the slide. The remaining FISH
590 procedure followed the original protocol[63].

591 Immunostaining and FISH on E6.5 embryos

592 Following natural mating, embryos were dissected at E6.5 as described above. After
593 dissection, the ectoplacental cones were removed using 27G needles, and embryos were
594 washed in three drops of 1x PBS to avoid contamination of maternal tissues. Embryonic cells
595 were then spread on microscopy slides in the fixative solution (4% PFA and 0.01% Tween-20
596 in 1x PBS). Cells were mechanically dissociated by pipetting up and down using a mouth-
597 operated pipette. The PFA solution was allowed to dry, and the slides were frozen at -20°C.
598 Each embryo was spread within a ring made with rubber cement (Elmer's, cat# E904) on the
599 slide using a 1 ml syringe with a 27G needle.

600 For immunostaining, slides were thawed and briefly washed three times in 1x PBS and
601 incubated in the blocking solution (10% BSA, 0.01% Tween-20 in 1x PBS) for 1 hour at RT
602 in a humidified chamber. The slides were then incubated with a rabbit anti-human 53BP1
603 antibody (Fig. 4a, 1:2000, Invitrogen, cat# PA1-16565) for 1 hour at RT, washed three times
604 with 1x PBS for 10 min, incubated with Alexa Fluor 647–conjugated donkey anti-rabbit
605 (1:500, Invitrogen, cat# A32795) in the blocking solution (2% BSA, 0.01% Tween-20 in 1x
606 PBS), and washed three times with 1x PBS for 10 min. Rubber cement rings were removed
607 using a fine tweezer, and slides were mounted with Antifade Mounting Medium with DAPI.
608 After imaging the immunostained slides, coverslips were removed by immersion in 1x PBS

609 to proceed to the Oligopaint FISH process. Slides were washed for 10 min in 1x PBS,
610 dehydrated in ethanol series (85%, 90%, 100%), air-dried, and aged at RT for one day. Slides
611 were fixed with 1% paraformaldehyde in 1x PBS for 10 min at RT, washed for 5 min with 1x
612 PBS at RT, dehydrated in ethanol series, air dried, and the primary Oligopaint mix[63] with 100
613 pmol of the HSR probe was mounted to the slides and sealed with rubber cement. Subsequent
614 steps were performed as described in Clark et al[63].

615 Plasmid construction and cRNA synthesis

616 Plasmids were synthesized by Twist Bioscience using the plasmid In Vitro Transcription
617 (pIVT) vector[64] with N-terminal EGFP for SP100-rs, SP100, SP110, and SP140 constructs
618 and pIVT with N-terminal mCherry for the SP110 construct. Plasmid DNA linearized by
619 NdeI (New England Biolabs, cat# R0111S) were used as a template to synthesize cRNAs
620 with the T7 mMessage mMachine Kit (Ambion, cat# AM1340), followed by purification
621 using the MEGAclear Kit (ThermoFisher, cat# AM1908). cRNAs were diluted in nuclease-
622 free water to adjust their concentrations for microinjection (see below).

623 Zygote microinjection and immunostaining

624 Zygotes were microinjected with cRNA in M2 media using a piezo-driven micromanipulator,
625 piezoXpert (Eppendorf). During microinjection, zygotes with abnormal pronuclei numbers
626 and unfertilized eggs were discarded. Following the microinjection, zygotes were cultured to
627 different stages at 37°C in a humidified atmosphere of 5% CO_2 in air. cRNAs used in this
628 study were *Egfp-Sp100-rs* (*M. m. domesticus* SP100-rs with EGFP at the N-terminus) at 1743
629 ng/µl, *Egfp-Sp100* (*M. m. domesticus* SP100 (isoform 1) with EGFP at the N -terminus) at
630 62.5, 90, 125, 250, and 1767 ng/µl, *Egfp-Sp110* (*M. m. domesticus* SP110 with EGFP at the
631 N-terminus) at 125 ng/µl, *mCherry*-Sp110 (*M. m. domesticus* SP110 with mCherry at the N-
632 terminus) at 125 and 250 ng/µl, and *Egfp-Sp140* (*M. m. domesticus* SP140 with EGFP at the
633 N-terminus) at 125 and 250 ng/µl. cRNAs used in co-injections were *Egfp-Sp100* at 90 ng/µl
634 and *mCherry-Sp110* at 125 ng/µl or *Egfp-Sp100* at 125 ng/µl and *mCherry-Sp110* at 250
635 ng/µl. After culturing, embryos were imaged at E1.5 or E4.5 to examine protein expression
636 levels. Subsequently, embryos were fixed in freshly prepared 2% paraformaldehyde in 1x
637 PBS with 0.1% Triton X-100 for 20 min at RT, washed in blocking solution (0.3% BSA and
638 0.01% Tween-20 in 1x PBS) for 10 min at RT, permeabilized in 1x PBS with 0.1% Triton X-
639 100 for 15 min at RT, incubated in the blocking solution (5% BSA and 0.01% Tween-20 in 1x
640 PBS) for 1 hour at RT, incubated 1 hour with rabbit anti-human 53BP1 antibody (Fig. 4b,c,
641 1:2000, Invitrogen, cat# PA1-16565) at RT, washed three times for 10 min with the blocking
642 solution (5% BSA and 0.01% Tween-20 in 1x PBS), incubated 1 hour with Alexa Fluor 647–
643 conjugated donkey anti-rabbit (1:500, Invitrogen, cat# A32795) antibody at RT, washed three
644 times for 10 min in the blocking solution (0.3% BSA and 0.01% Tween-20 in 1x PBS),
645 incubated 30 min with Antifade Mounting Medium with DAPI (Vector Laboratories, cat# H-
646 1200) diluted 1:1 in the blocking solution, and placed into 3 µl drops of the blocking solution
647 covered with paraffin oil in a glass-bottom tissue culture dish (fluoroDish, cat# FD35–100) to
648 proceed to confocal microscopy (see below).

649 Microscopy and image analysis

Fixed oocytes and embryonic cells were imaged with a microscope (Eclipse Ti; Nikon) equipped with 20x / 0.75 NA objective and 100x / 1.40 NA oil-immersion objective lens, CSU-W1 spinning disk confocal scanner (Yokogawa), ORCA Fusion Digital CMOS camera (Hamamatsu Photonics), and 405, 488, 561 and 640 nm laser lines controlled by the NIS-Elements imaging software (Nikon). Confocal images were acquired as Z-stacks at 1 or 3 µm intervals. Fixed oocytes and embryos were imaged with a microscope (Eclipse Ti2-E; Nikon) equipped with the 20x / 0.75 NA objective and 60x / 1.40 NA oil-immersion objective, CSU-W1 spinning disk confocal scanner (Yokogawa), ORCA Fusion Digital CMOS camera (Hamamatsu Photonics), and 405, 488, 561 and 640 nm laser lines controlled by the NIS-Elements imaging software (Nikon). Confocal images were collected as Z-stacks at 0.5, 1, or 3 µm intervals. Fiji/ImageJ (NIH) was used to analyze all the images. In general, optical slices containing nuclei or cells were added to produce a sum intensity Z-projection for pixel intensity quantifications. For quantifications of foci, optical slices were added to produce a sum (Fig. 4a) or maximum intensity Z-projection (Fig. 4b,c).

To quantify H3K9me3 signal intensities at the HSR locus (Fig. 2f), regions of interest (ROIs) were drawn to encompass the H3K9me3 signal on the chromosome 1 arm. In general, H3K9me3 signals are enriched at the centromeric region of each chromosome, and the only H3K9me3 focus outside the centromere corresponds to the HSR locus. The signal intensity was integrated over each ROI after subtracting background signals, obtained from the average of three chromosome regions near the HSR locus.

To quantify SP100 nucleoplasmic signal intensities in meiosis I GV oocytes and two-cell embryos (Fig. 3a), ROIs were drawn encompassing the SP100 nuclear signal based on the DAPI staining. The signal intensity was integrated over each ROI after subtracting background signals, obtained from the background outside the cell. To quantify SP100 and SP140 total signal intensities in meiosis II eggs and two-cell embryos (Fig. 3b and Extended Data Fig. 6a), ROIs were drawn encompassing the entire cell. The signal intensity was integrated over each ROI after subtracting background signals, obtained from three background areas outside the cell. To quantify nucleoplasmic signal intensities in two-cell embryos (Fig. 3b), masking images were created using DAPI staining images to specifically measure signal intensities in the nucleus. The signal intensity was integrated over each slice after subtracting background signals, obtained from three background areas outside of the cell. To quantify nucleoplasmic signal intensities (SP100 and SP110) in IF-FISH images (Fig. 3c and Extended Data Fig. 3), masking images were created using DAPI staining images to specifically measure signal intensities in the nucleus. Signal intensity was averaged over each slice after subtracting cytoplasmic background signals. Nucleoplasmic signals of EGFP-SP100 (Fig. 4c) were quantified by the same method.

To quantify 53BP1 foci number per cell (Fig. 4a), we developed a custom ImageJ/Fiji macro (Supplementary Method 1) based on the strategy developed by the Duke Light Microscopy Core (https://microscopy.duke.edu/guides/count-nuclear-foci-ImageJ). We manually counted 53BP1 foci number in Fig. 4b,c, using maximum-intensity projected images. Foci with ≥ 1 µm diameter were counted. We analyzed each slice when nuclei from different cells overlap.

691 Embryo transfer

692 Embryo transfers were performed by the NHLBI Transgenic Core at NIH. In the first embryo
693 transfer experiment (Fig. 1g), +/+ zygotes were collected from +/+ females mated with +/+
694 males and cultured for one day to reach the two-cell stage. Two-cell embryos were then
695 transferred to pseudo-pregnant H/+ *dom* females (mated with vasectomized males prior to the
696 transfer). As a control, embryos were also transferred to pseudo-pregnant +/+ females.
697 Embryos were dissected from these females at E9.5 (two +/+ and three H/+ females). The
698 number of live embryos and resorbing sites were scored to quantify embryo survival rates in
699 the H/+ and +/+ uterus. A replica of this experiment was performed, and the embryos were
700 dissected at E13.5 and E17.5 (three +/+ and three H/+ females for each timepoint).

701 In a second embryo transfer experiment (Fig. 1h), a mixture of +/+ and H/+ two-cell embryos
702 obtained by crossing H/+ *dom* females with +/+ *dom* males were transferred to eight +/+
703 pseudo-pregnant *dom* females (CD-1 background). Embryos were dissected at E13.5 and
704 genotyped by qPCR as previously described. In a replica of this experiment, two-cell
705 embryos were implanted into five pseudo-pregnant females and dissected and genotyped at
706 E14.5.

707 Gene expression profiling by RT-qPCR

708 Quantification of expression levels of *Sp100*, *Sp110*, *Sp140*, and *Sp100-rs* genes were
709 performed using liver and oocytes of *M. m. domesticus* and *M. m. musculus.* Dissected tissues
710 were immediately frozen in liquid nitrogen and stored at -70°C. RNA from oocytes was
711 extracted using the TRIzol Reagent (Invitrogen, cat# 15596026) and from liver using the total
712 RNA extraction kit (Norgen, cat#17200). RNA integrities were examined on 1% agarose gels.
713 RNA purities were examined using the NanoPhotometer NP80 (Implen, cat# NC2831907).
714 cDNA for each sample was synthesized using the SuperScript™ III First-Strand Synthesis
715 System (Invitrogen, cat# 18080051) using 0.8 µg per sample of total RNA, following the
716 manufacturer's instructions. Working solutions of the obtained cDNAs were produced by
717 diluting them 1:5 in RNase-DNase free water.

718 Primers were designed using a modified version of Primer3[60] implemented in Geneious
719 10.2.6. Primer sets for *Sp100*, *Sp110*, *Sp140*, and *Sp100-rs* genes (Supplementary Table 1)
720 were designed spanning an exon-exon junction of each gene. Primer specificities were
721 confirmed using the Blast algorithm for short sequences[60,65]. *Sp100-rs* gene is a chimeric
722 gene with the first three exons of *Sp100* fused with *Csprs* gene. To specifically amplify
723 *Sp100-rs*, we designed a primer set spanning the junction of the 3rd exon of *Sp100* and the
724 exon of *Csprs*, which avoids amplifying *Sp100* (Extended Data Fig. 5c). Quantitative PCR
725 was performed on QuantStudio 3 (Applied Biosystems, cat# A28567), except for *Sp140* in
726 *dom* oocytes samples that were performed on LightCycler 96. Reactions were assembled in a
727 final volume of 10 µl with 1 µl of cDNA, 5 µl of iTaq Universal SYBR Green Supermix
728 (Bio-Rad, cat# 1725121), and 0.5 µl of each 10 µM primer. Cycle conditions were 95°C for
729 10 min; 40 cycles of 95°C for 5 s and 60°C for 20 s. The specificity of the PCR products was
730 confirmed by dissociation curve analysis. Target and reference genes were analyzed
731 simultaneously in triplicates for independent samples. DNA contamination was examined

using controls without reverse transcriptase (NRTC) and without template cDNA (NTC). A five-fold serial dilution of the cDNAs was used to calculate the primer sets amplification efficiency (E). An efficiency range of 90% to 110% was used to select primer sets for further analysis. Cq values were corrected using the gene's efficiencies with the formula CqE = Cq*(log(1+E)/log(2))[66]. The normalized relative expression quantity (NREQ) was determined by the $2^{-\Delta\Delta C_T}$ method[67]. Expression levels of target genes were normalized using the geometric mean of two housekeeping reference genes with subsequent normalization to the average expression of the +/+ group. To select the reference genes, we used the RefFinder[68] software. From five tested genes (*Atp5b*, *Gapdh*, *Hprt1*, *Rplpo*, and *Ubc*), we selected *Atp5b* and *Rplpo* for *dom* liver, *Atp5b* and *Gapdh* for *mus* liver, *Atp5b* and *Hprt1* for *dom* and *mus* oocytes.

Quantification and statistical analysis

Data points were pooled from two to five independent experiments in most experiments, and the exact number of independent experiments for each experimental group is listed in Supplementary Table 2. Data was analyzed using Microsoft Excel and GraphPad Prism 10. Bar graphs, scatter plots, and violin plots were created with GraphPad Prism 10. Binomial test (two-sided) for deviations from the expected 50:50 (Fig. 1d, Table 1) or the biasing cross ratio (Fig. 1h), Chi-square test (two-tailed) (Fig. 1g, Table 2), Mann-Whitney test (two-sided) (Fig. 1e, f, 2b-e, 3a, b nucleoplasmic, 3c, 4a, Extended Data Fig. 3, 6a), and Welch's t test (two-sided) (Fig. 2f, 3b total, 4c) were used for statistical analyses. Actual *P* values are shown in each figure or figure legend.

Data availability

The microscopy and western blot data required to reproduce the results in the current study will be publicly available in Figshare upon publication. Any additional information required to reanalyze the data reported in this paper is available from the corresponding authors upon request.

Acknowledgments

We thank M. Lichten for comments on the manuscript, Akera lab members for discussion, N. Altan-Bonnet, Y. Mukoyama, N. Mizuno, J.R. Hogg, and K. Sadtler for access to their laboratory equipment, G. Arora, R. Pavani, F.E. Clark, L.F. Rosin, V. Sundaresan, and W. Li for technical advice, A. Nussenzweig for the 53BP1 antibody, R.E. Vance for the SP140 antibody, NHLBI Transgenic Core (C. Liu) for embryo transfer experiments, and NIH building 14F animal facility staff for the care with our mouse colony, especially the "jumpy" mice. This work was funded by the Division of Intramural Research at the National Institutes of Health/National Heart, Lung, and Blood Institute, 1ZIAHL006249 to TA. The contributions of the NIH authors are considered Works of the United States Government. The findings and conclusions presented in this paper are those of the authors and do not necessarily reflect the views of the NIH or the U.S. Department of Health and Human Services.

Author contributions

Conceptualization: D.M.Z.A.S. and T.A. Methodology: D.M.Z.A.S., M.S., and T.T. Investigation: D.M.Z.A.S., M.S., T.T., and T.A. Funding acquisition: T.A. Supervision: T.A. Writing—original draft: D.M.Z.A.S. Writing—review and editing: D.M.Z.A.S., M.S., T.T., and T.A.

Competing interests

The authors declare no competing interests.

Materials & Correspondence

Correspondence and requests for materials should be addressed to Duilio M.Z.A. Silva or Takashi Akera.

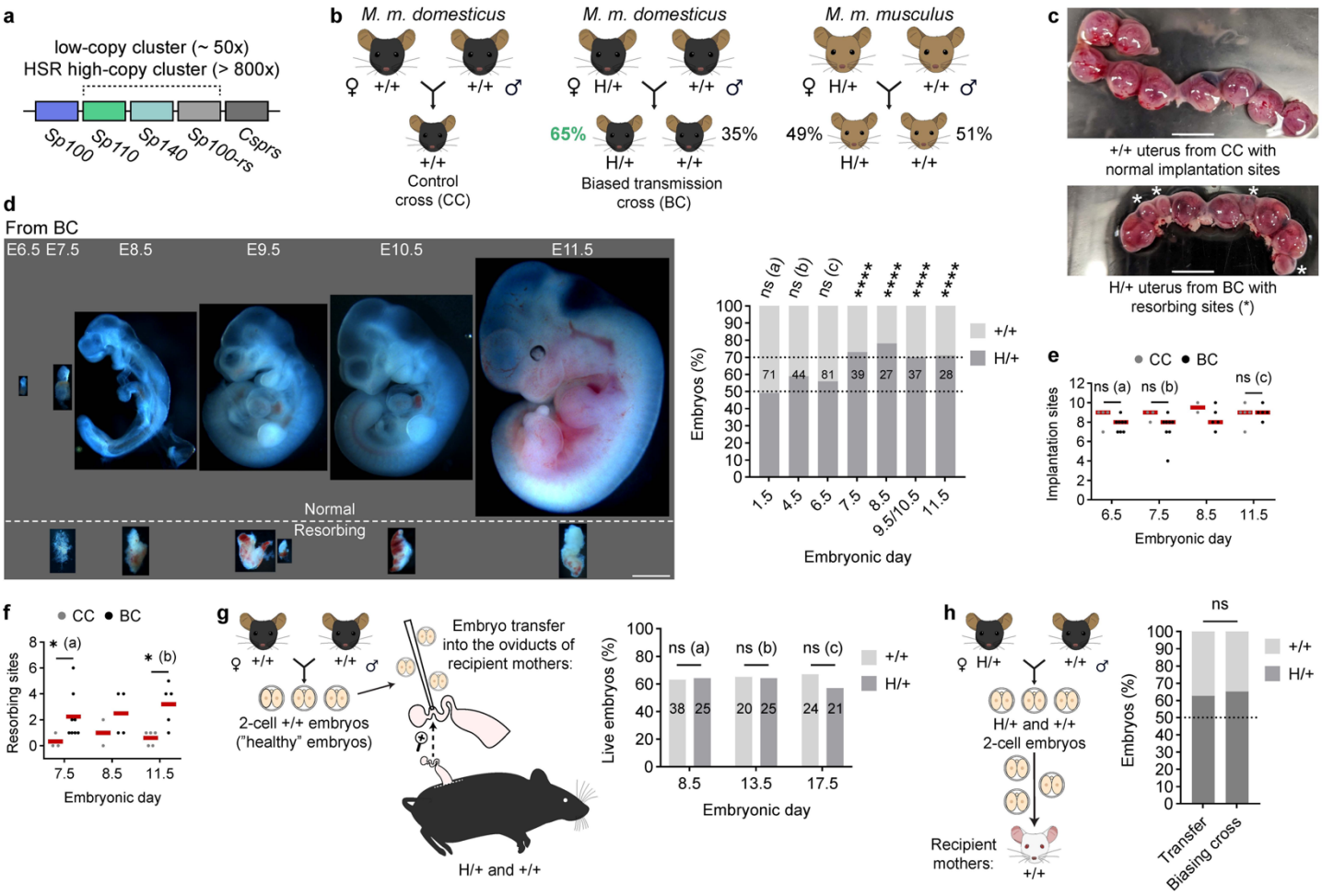

Fig. 1. Selfish HSR kills wild-type embryos by causing internal issues. a, Simplified diagram of the HSR locus (high-copy repeat) and wild-type low-copy repeat based on Weichenhan, D. et al[69]. **b**, Schematic of different crosses to study HSR transmission. **c**, Uterus from the control cross (CC) with regular implantation sites and from the biasing cross (BC) with resorbing sites (*); scale bars, 500 μm. **d**, Time-course embryo dissection showing normal and resorbing embryos from the biasing cross; E, embryonic day; scale bar, 1 mm. Graph is a quantification of genotype ratios (H/+ versus +/+) at each time point; total number of embryos analyzed are indicated on top of each bar; Binomial test (two-sided) was used to examine deviation from the Mendelian expectation (50:50); ns (a) = 0.9204, ns (b) =0.0886, ns (c) = 0.2713, ****$P < 0.0001$. **e**, Numbers of implantation sites in the control cross (CC) and the biasing cross (BC) were quantified; n = 4, 8, 3, 8, 2, 5, 5, and 5 females from left to right groups; Mann-Whitney test (two-sided) was used for statistical analysis; ns (a) = 0.2788, ns (b) = 0.1636, ns (c) = 0.9524. **f**, Numbers of resorbing sites in CC and BC were quantified; n = 3, 8, 2, 4, 5, and 5 females for E6.5 CC, E6.5 BC, E7.5 CC, E7.5 BC, E8.5 CC, E8.5 BC, E11.5 CC, and E11.5 BC, respectively; Mann-Whitney test (two-sided) was used for statistical analysis; * (a) $P = 0.0485$, * (b) $P = 0.0317$. **g**, Schematic of the first embryo transfer experiment using healthy two- cell embryos from CC (left); percentages of live embryos relative to total implantation sites were quantified for each recipient mother's genotype, +/+ and H/+, at different timepoints; number of embryos analyzed is indicated on top of each bar; Chi-square test (two-sided) was used for statistical analysis; ns (a) = 0.9458,

806 ns (b) = 0.9445, ns (c) = 0.5109. **h**, Schematic of the second embryo transfer experiment
807 using two-cell embryos from BC (left); The genotype ratio of transferred embryos was
808 compared to natural biasing cross (the data for natural cross is from Table 1); n = 51, 287;
809 Binomial test (two-sided) was used for statistical analysis; ns = 0.7692.

810

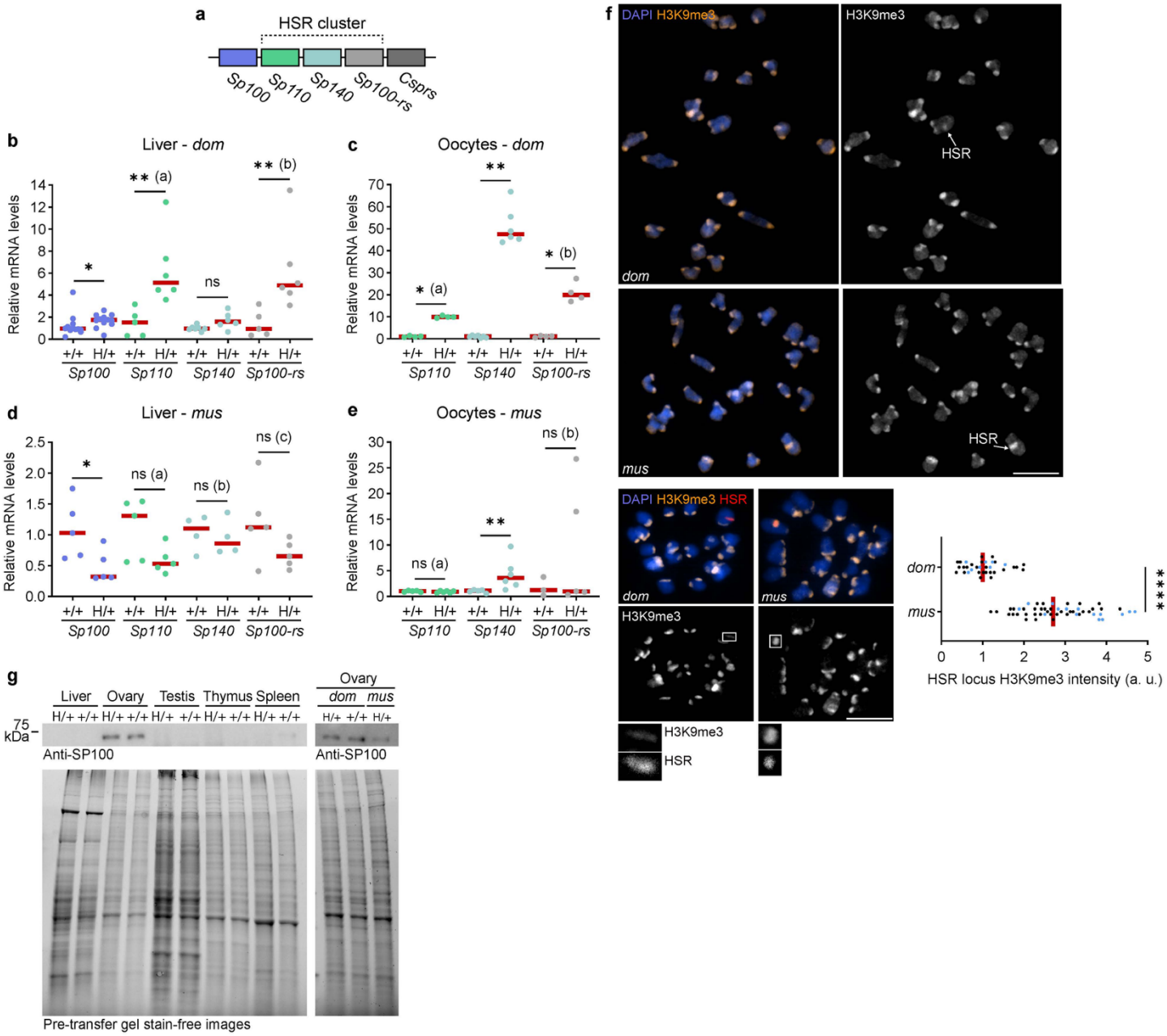

Fig. 2. No HSR gene expression, no biased transmission. a, Simplified diagram of HSR repeats based on Weichenhan, D. et al[69]. **b**, Transcript levels of HSR genes in +/+ and H/+ *Mus musculus domesticus* (*dom*) liver were analyzed by RT-qPCR; Mann-Whitney test (two-sided) was used for statistical analysis; n = 12, 12, 5, 6, 7, 6, 5, and 6 for samples from left to right groups. Data for *Sp100* was pooled from two independent experiments. * $P = 0.0242$, ** (a) $P = 0.0043$, ns = 0.0513, ** (b) $P = 0.0087$; red line, median. **c**, Transcript levels of HSR genes in +/+ and H/+ *dom* oocytes analyzed by RT-qPCR; Mann-Whitney test (two-sided) was used for statistical analysis; n = 4, 4, 7, 6, 4, and 4 for samples from left to right groups. * (a) $P = 0.0286$, ** $P = 0.0012$, * (b) $P = 0.0286$; red line, median. **d**, Transcript levels of HSR genes in +/+ and H/+ *Mus musculus musculus* (*mus*) liver analyzed by RT-qPCR; Mann-Whitney test (two-sided) was used for statistical analysis; n = 5, 5, 5, 5, 4, 4, 5, and 5 for samples from left to right groups. * $P = 0.0317$, ns (a) $P = 0.0952$, ns (b) $P = 0.8857$, ns (c) $P = 0.1508$; red line, median. **e**, Transcript levels of HSR genes in +/+ and H/+ *mus* oocytes

824 analyzed by RT-qPCR; Mann-Whitney test (two-sided) was used for statistical analysis; n =
825 5, 6, 5, 6, 3, and 5 for samples from left to right groups. ns (a) = 0.329, **P = 0.0087, ns (b) =
826 0.7857; red line, median. In b-e**,** comparisons are made within each gene, and the values are
827 not intended for comparisons across different genes. **f**, H/+ oocytes from *dom* and *mus* were
828 fixed at prometaphase I and stained for H3K9me3 (top). H3K9me3 signal intensities at the
829 HSR locus were quantified; datapoints from two independent experiments are indicated by
830 dots with distinct colors; n = 34 and 51 for *dom* and *mus*, respectively; Welch's t test (two-
831 sided) was used for statistical analysis; ****$P < 0.0001$; red line, median. Images are sum
832 intensity Z-projections showing all chromosomes; scale bar, 10 μm. H/+ oocytes from *dom*
833 and *mus* were fixed at prometaphase I and stained for H3K9me3, followed by FISH using the
834 HSR probe (bottom). Images are sum intensity Z-projections showing all chromosomes; scale
835 bar, 10 μm, scale bar of enlarged insets, 1 μm. **g**, Western blot of SP100 using tissue samples
836 from H/+ and +/+ *dom* (left) and *dom* and *mus* (right). As a loading control, stain-free gel
837 images are shown; see Extended Data Fig. 2 for gel source data.

838

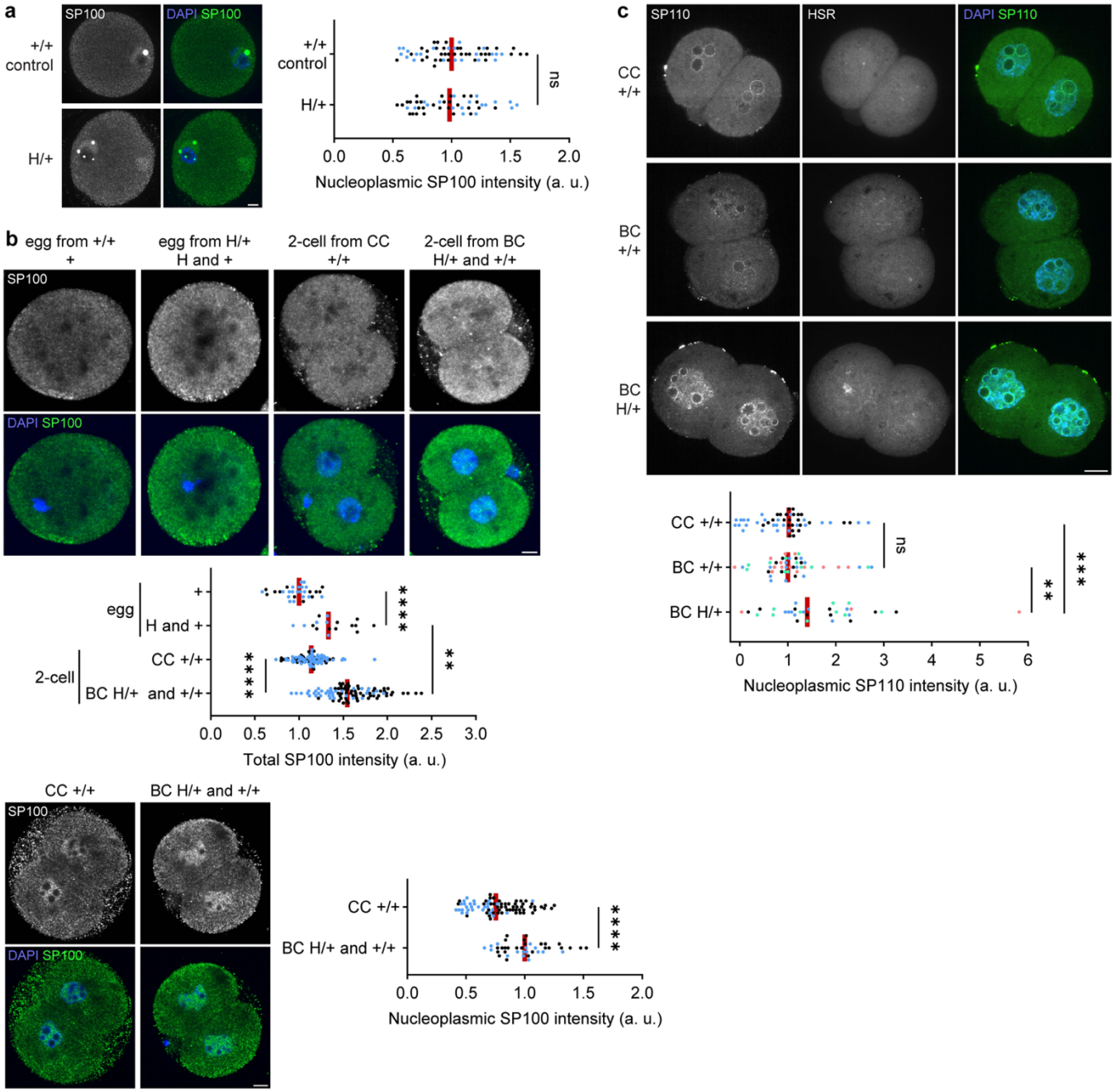

Fig. 3. Toxin is deposited in all embryos while the antidote is private to HSR embryos. a, Oocytes were fixed at the germinal vesicle (GV) stage and stained for SP100. The signal intensities were quantified; n = 58 and 47 for +/+ control and H/+, respectively; Mann-Whitney test (two-sided) was used for statistical analysis; ns = 0.3912; red line, median; dots, individual cells from two-cell embryos. Images are maximum intensity Z-projections; scale bar, 10 μm. **b**, metaphase II eggs and two-cell embryos were fixed and stained for SP100. The total signal intensities in each cell were quantified (top) (n = 31, 17, 100, and 92 for + egg, H, and + egg, CC +/+ 2-cell, BC H/+ and +/+ 2-cell, respectively). Welch's t test (two-sided) was used for statistical analysis; ****$P < 0.0001$, **$P = 0.0063$; red line, median; dots, individual cells. Nucleoplasmic signal intensities were quantified in two-cell embryos (bottom) (n = 80, and 42 for CC +/+, and BC H/+ and +/+, respectively); Mann-Whitney test (two-sided) was used for statistical analysis; ****$P < 0.0001$; red line, median; dots,

individual cells. Images are maximum intensity Z-projections; scale bar, 10 μm. **c**, Embryos were fixed at the late two-cell stage, stained for SP110, and genotyped by FISH with the HSR probe. The signal intensities were quantified (n = 50, 47, and 33 for +/+ CC, +/+ BC, and H/+ BC, respectively). Mann-Whitney test (two-sided) was used for statistical analysis; ns = 0.3368, $^{**}P = 0.0037$, $^{***}P = 0.0004$; red line, median; dots, individual cells. This experiment was repeated independently two times for +/+ CC and four times for +/+ and HSR/+ BC (depicted by the colors of the dots) with similar results. Images are maximum intensity Z-projections; scale bar, 10 μm. Data points from two or more independent experiments are indicated by dots with distinct colors.

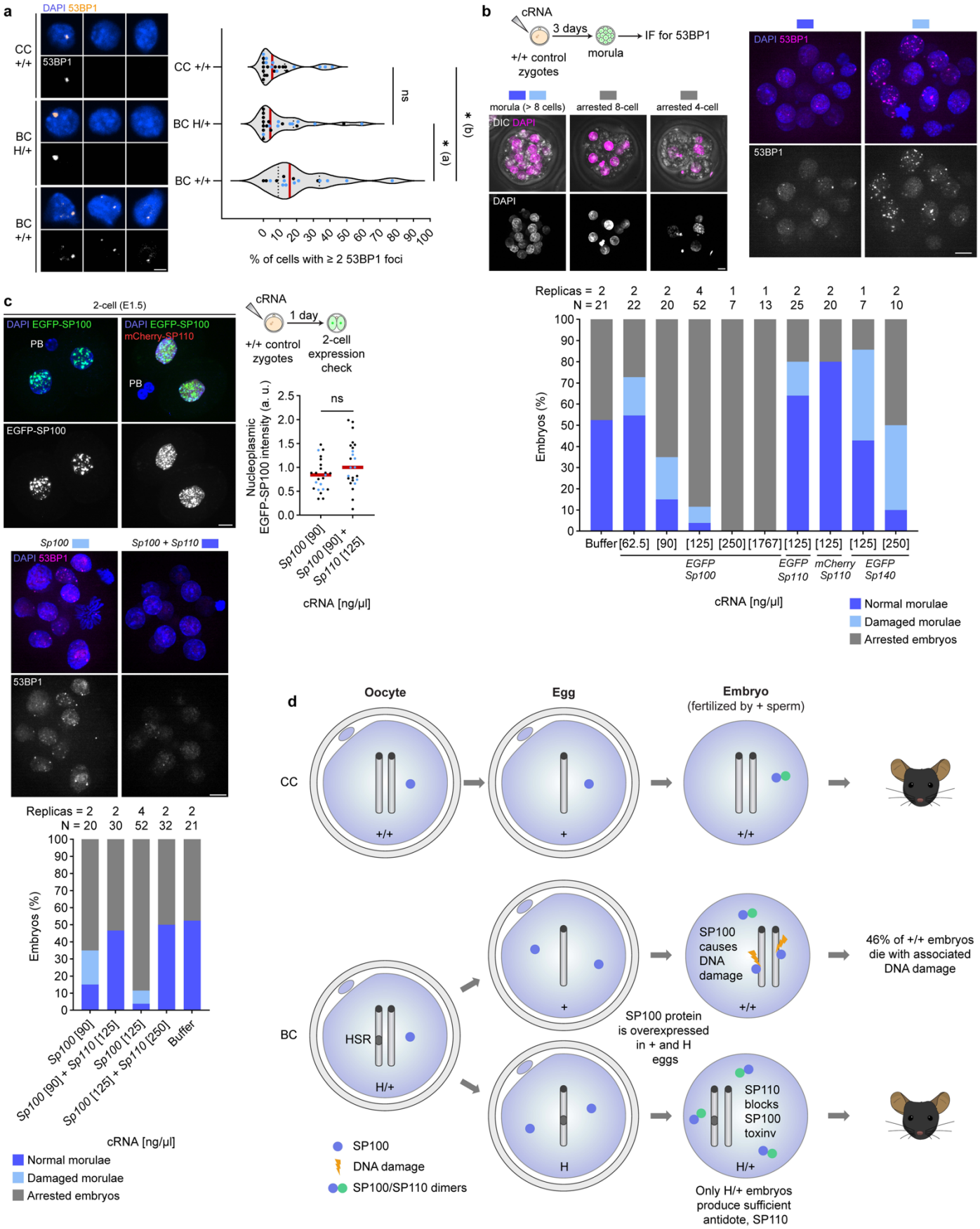

Fig. 4. SP100 and SP110 consist a minimal toxin-antidote system, sabotaging mammalian embryogenesis. a, Embryos from control cross (CC) and biasing cross (BC)

were fixed at E6.5 and stained for 53BP1. Percentages of cells with more than two 53BP1 foci in each embryo were quantified; Mann-Whitney test (two-sided) was used for statistical analysis; ns = 0.9691, * (a) $P = 0.0254$, * (b) $P = 0.0102$; red line, median; dots, percentage per embryo. Data points from two independent experiments are indicated by dots with distinct colors (n = 24, 22, 16 embryos for +/+ CC, H/+ BC, and +/+ BC, respectively). **b**, Zygotes were microinjected with cRNA, cultured for three days (E3.5), and fixed to stain for 53BP1. Embryos at the morula stage (> eight cells) were classified as normal morulae (< two cells within the embryo with five or more 53BP1 foci, dark blue) or damaged morulae (two or more cells with five or more 53BP1 foci, light blue), and embryos with eight cells or fewerwere classified as arrested embryos (grey). Proportions of embryos in each category were quantified; sample size and the number of independent experiments are shown above each bar in the graph. **c**, Embryos expressing EGFP-SP100 and mCherry-SP110 were fixed at the two-cell stage and counterstained with DAPI. EGFP-SP100 nucleoplasmic signal intensities were quantified as a readout of expression levels; datapoints from two independent experiments are indicated by dots with distinct colors; n = 23 and 24 for *Sp100* [90] and *Sp100* [90] + *Sp110* [125], respectively; Welch's t test (two-sided) was used for statistical analysis; ns = 0.0625; red line, median; dots, individual cells. Similarly, embryos expressing EGFP-SP100 and mCherry-SP110 were cultured for three days, fixed and stained for 53BP1, and categorized as in **b** (bottom); note that data for *Sp100* [90], *Sp100* [125], and Buffer are from the graph in **b**; sample size and the number of independent experiments are shown above each bar. Images in this figure are maximum intensity Z-projections except for the ones with DIC, which are standard deviation intensity Z-projections; PB, polar body; scale bar, 10 μm. **d**, Schematic of the HSR toxin-antidote elements system.